

Topology Optimization Design of 3D Continuum Structure with Reserved Hole Based on Variable Density Method

Bai Shiye and Zhu Jiejiang

The Department of Civil engineering, Shanghai University, Shanghai 200072, China

Received 25 February 2016; Accepted 22 May 2016

Abstract

An objective function defined by minimum compliance of topology optimization for 3D continuum structure was established to search optimal material distribution constrained by the predetermined volume restriction. Based on the improved SIMP (solid isotropic microstructures with penalization) model and the new sensitivity filtering technique, basic iteration equations of 3D finite element analysis were deduced and solved by optimization criterion method. All the above procedures were written in MATLAB programming language, and the topology optimization design examples of 3D continuum structure with reserved hole were examined repeatedly by observing various indexes, including compliance, maximum displacement, and density index. The influence of mesh, penalty factors, and filter radius on the topology results was analyzed. Computational results showed that the finer or coarser the mesh number was, the larger the compliance, maximum displacement, and density index would be. When the filtering radius was larger than 1.0, the topology shape no longer appeared as a chessboard problem, thus suggesting that the presented sensitivity filtering method was valid. The penalty factor should be an integer because iteration steps increased greatly when it is a non-integer. The above modified variable density method could provide technical routes for topology optimization design of more complex 3D continuum structures in the future.

Keywords: Topology Optimization, Reserved Hole, Multiple Loading Conditions, Variable Density Method, MATLAB

1. Introduction

Topology optimization design is a computational method for achieving optimal material distribution without knowing the special shape of the structure in advance. Therefore, topology optimization can be used to develop great potential of new structure with high performance. The history of the topology optimization dates back to the truss theory proposed by Michell in 1904. At that time, the theory can only be applied to single working condition that depended on the strain filed and was not applicable in practical engineering [1]. In 1964, Dorn et al. proposed ground structure approach [2] that was applied into topology optimization. From then on, topology optimization had become a more active research field. In recent years, topology optimization theory of continuum structure [3] has developed rapidly. Many topology optimization methods including variable thickness method, variable density method, asymptotic structure optimization, independent continuum mapping method (ICM), level set, and nodal density method [4] have been proposed. Topology optimization methods have been applied in many fields.

Especially the variable density method has been successfully applied in many practical engineering projects because of its simple programming procedure and high efficiency in calculation competence [5]. Yang et al. transformed topology optimization problems into linear programming problems and then used the variable density method to design engine components [6]. With the

development of many CAE software based on the variable density method, the engineering examples of topology optimization that are solved by numerical simulation methods have increased daily [7], [8], [9], [10], [11], [12].

2. State of the Art

Numerical instability problems including chessboard and mesh dependence phenomenon are ubiquitous in topology optimization design based on variable density method [13]. Sigmund proposed a filtering radius method to solve this problem [14]. Zuo modified the previous filtering method [15]. Chen used an adjacent entropy filtering method based on graph theory to eliminate the chessboard and mesh dependence problems [16].

The essence of topology optimization is to solve the extrema problem. Therefore, the development of topology optimization is inseparable from optimal mathematical algorithms. The advantage of the optimization criterion method (OC method) is fast convergence speed, however, this method might be difficult to deal with the complex structure under the conditions of different constraints [17]. In 1960, Schmit adopted mathematical programming theory to solve optimization problems of elastic structure under the condition of multiple load [18]. His research pushed the development and application of topology optimization algorithms. Traditional optimization methods are not applicable for these problems because mathematical models are complicated, nonlinear, random, and blurry in real optimization design problems. Therefore, many new algorithms, including simulated annealing method [19],

* E-mail address: bai880602@sina.com

genetic algorithm [20], evolutionary algorithm [21], and neural network algorithm [22], [23], were presented. Based on the above modern methods, the global or approximately global solutions can generally be obtained. However, this will cost huge amount of calculation time. The minimum compliance problem in nonlinear programming can be dealt with by sequential quadratic programming (SQP) [24], [25] and moving asymptotes method (MMA) [26], [27]. Compared with SQP and MMA methods, the OC method has many advantages including good computation convergence and fast computation speed in topology optimization design. Hence, in this study, the OC method is used to solve the minimum compliance problem of the topology optimization model.

The remainder of this study is organized as follows. Section 3 establishes a 3D topology optimization model of continuum structure with the object function of minimum compliance and deduces the 3D finite element formulations by OC method. Section 4 studied the topology optimization design examples of 3D continuum structure with reserved hole and discusses the influence of mesh numbers, penalty factor, and filtering radius on results of topology optimization. Section 5 presents conclusions.

3. Methodology

3.1 Minimum Compliance Problem

The minimum compliance problem of topology optimization design of the continuum structure constrained by volume fraction is expressed as follows:

$$\begin{aligned} \min C(x) \\ \left\{ \begin{aligned} V[x] &= \int_{\Omega} x d\Omega \leq V^* \\ 0 < x &\leq 1, V^* = \alpha V_0 \\ x &= 0 \text{ or } 1 \end{aligned} \right. \end{aligned} \quad (1)$$

where $C(x)$ is compliance of structure. x is material pseudo-density as the design variable. Ω is the given design domain. V^* is the required optimal design volume. V_0 is the original design volume. α is the volume fraction.

3.2 Newly Improved SIMP Model

The basic approach used to handle the problem of discrete variables in numerical calculation is to substitute continuous function for discrete function. The continuous function can generate many elements, and the continuous density of which is between 0 and 1. However, making this kind of structure material practical is difficult. To solve this problem, the penalty factor is usually introduced to suppress the appearance of intermediate-density element. By using variable density method and introducing penalty factor, the relationship between variable density x_i and elasticity modulus E_i based on SIMP model is expressed as follows:

$$E_i = E_i(x_i) = x_i^p E_0, \quad x_i \in [0,1] \quad (2)$$

where E_0 is elasticity modulus of solid materials. p is the penalty factor. The evolved solid isotropic microstructures with penalization (SIMP) model are expressed as follows:

$$E_i = E_i(x_i) = E_{\min} + x_i^p (E_0 - E_{\min}), \quad x_i \in [0,1] \quad (3)$$

where E_{\min} is the elasticity modulus of void material. To avoid the singularity of the stiffness matrix, the value is not zero as usual. The value is set to "0.001." The improved SIMP model makes the penalty factor and elasticity modulus of void material mutually independent. Compared with the former model, the improved SIMP model has better convergence in computation [28].

3.3 Sensitivity Filtering

Topology optimization model based on variable density method is always accompanied with numerical problems, such as mesh-dependence, checkerboard pattern, local extremum, and so on. To solve these problems, the common way is to introduce density-filtering method shown as follows:

$$\bar{x}_i = \frac{\sum_{j \in N_i} H_{ij} v_j x_j}{\sum_{j \in N_i} H_{ij} v_j} \quad (4)$$

where v_i is the volume of element. H_{ij} is the weighting factor. N_i is the element set adjacent to element i and can be defined as

$$N_i = \{j : dist(i, j) \leq R\} \quad (5)$$

where the operator $dist(i, j)$ is the center distance between element i and element j , and R is the filtering radius. The weighting factor H_{ij} is:

$$H_{ij} = R - dist(i, j) \quad (6)$$

Filtering density \bar{x}_i is modified density. This factor is introduced into the SIMP model, and the formula can be deduced as follows:

$$E_i(\bar{x}_i) = E_{\min} + \bar{x}_i^p (E_0 - E_{\min}), \quad \bar{x}_i \in [0,1] \quad (7)$$

3.4 Element Stiffness Matrix and Formulation of Finite Element

Based on improved SIMP model, as indicated in Formula (7), sensitivity filtering method, and Hooke's Law, the 3D stress matrix of isotropic material element i is expressed as:

$$D_i(\bar{x}_i) = E_i(\bar{x}_i) D_i^0, \quad \bar{x}_i \in [0,1] \quad (8)$$

where D_i^0 is the stress matrix composed of unit Young's modulus and can be expressed as:

$$D_i^0 = \frac{1}{(1+\nu)(1-2\nu)} \times \begin{bmatrix} 1 & \nu & \nu & \nu & 0 & 0 & 0 \\ \nu & 1 & \nu & \nu & 0 & 0 & 0 \\ \nu & \nu & 1 & \nu & 0 & 0 & 0 \\ 0 & 0 & 0 & (1-2\nu)/2 & 0 & 0 & 0 \\ 0 & 0 & 0 & 0 & (1-2\nu)/2 & 0 & 0 \\ 0 & 0 & 0 & 0 & 0 & (1-2\nu)/2 & 0 \end{bmatrix} \quad (9)$$

where ν is Poisson ratio of isotropic material. Based on finite element theory, the element stiffness matrix of elastic

solid is the volume integral of stress matrix $D_i(\bar{x}_i)$ and strain matrix B , which can be expressed as follows:

$$k_i(\bar{x}_i) = \int_{-1}^{+1} \int_{-1}^{+1} \int_{-1}^{+1} B^T D_i(\bar{x}_i) B d\xi_1 d\xi_2 d\xi_3 \quad (10)$$

where $\xi_e (e=1,2,3)$ is the natural coordinate system of hexahedron element. Strain matrix B describes the relationship between the node displacement of elements and the strain. Based on SIMP model, the element stiffness matrix can be expressed as:

$$k_i(\bar{x}_i) = E_i(\bar{x}_i) k_i^0 \quad (11)$$

where

$$k_i^0 = \int_{-1}^{+1} \int_{-1}^{+1} \int_{-1}^{+1} B_i^T D_i^0 B d\xi_1 d\xi_2 d\xi_3 \quad (12)$$

Substituting Formula (9) into Formula (12), it can be further organized as:

$$k_i^0 = \frac{1}{(1+\nu)(1-2\nu)} \begin{bmatrix} \mathbf{k}_1 & \mathbf{k}_2 & \mathbf{k}_3 & \mathbf{k}_4 \\ \mathbf{k}_2^T & \mathbf{k}_5 & \mathbf{k}_6 & \mathbf{k}_4^T \\ \mathbf{k}_3^T & \mathbf{k}_6 & \mathbf{k}_5^T & \mathbf{k}_2^T \\ \mathbf{k}_4 & \mathbf{k}_3 & \mathbf{k}_2 & \mathbf{k}_1^T \end{bmatrix} \quad (13)$$

where

$$\begin{aligned} \mathbf{k}_1 &= \begin{bmatrix} k_1 & k_2 & k_2 & k_3 & k_5 & k_5 \\ k_2 & k_1 & k_2 & k_4 & k_6 & k_7 \\ k_2 & k_2 & k_1 & k_4 & k_7 & k_6 \\ k_3 & k_4 & k_4 & k_1 & k_8 & k_8 \\ k_5 & k_6 & k_7 & k_8 & k_1 & k_2 \\ k_5 & k_7 & k_6 & k_8 & k_2 & k_1 \end{bmatrix} & \mathbf{k}_2 &= \begin{bmatrix} k_9 & k_8 & k_{12} & k_6 & k_4 & k_7 \\ k_8 & k_9 & k_{12} & k_5 & k_3 & k_5 \\ k_{10} & k_{10} & k_{13} & k_7 & k_4 & k_6 \\ k_6 & k_5 & k_{11} & k_9 & k_2 & k_{10} \\ k_4 & k_3 & k_5 & k_2 & k_9 & k_{12} \\ k_{11} & k_4 & k_6 & k_{12} & k_{10} & k_{13} \end{bmatrix} \\ \mathbf{k}_3 &= \begin{bmatrix} k_6 & k_7 & k_4 & k_9 & k_{12} & k_8 \\ k_7 & k_6 & k_4 & k_{10} & k_{13} & k_{10} \\ k_5 & k_5 & k_3 & k_8 & k_{12} & k_9 \\ k_9 & k_{10} & k_2 & k_6 & k_{11} & k_5 \\ k_{12} & k_{13} & k_{10} & k_{11} & k_6 & k_4 \\ k_2 & k_{12} & k_9 & k_4 & k_5 & k_3 \end{bmatrix} & \mathbf{k}_4 &= \begin{bmatrix} k_{14} & k_{11} & k_{11} & k_{13} & k_{10} & k_{10} \\ k_{11} & k_{14} & k_{11} & k_{12} & k_9 & k_8 \\ k_{11} & k_{11} & k_{14} & k_{12} & k_8 & k_9 \\ k_{13} & k_{12} & k_{12} & k_{14} & k_7 & k_7 \\ k_{10} & k_9 & k_8 & k_7 & k_{14} & k_{11} \\ k_{10} & k_8 & k_9 & k_7 & k_{11} & k_{14} \end{bmatrix} \\ \mathbf{k}_5 &= \begin{bmatrix} k_1 & k_2 & k_8 & k_3 & k_5 & k_4 \\ k_2 & k_1 & k_8 & k_4 & k_6 & k_{11} \\ k_8 & k_8 & k_1 & k_5 & k_{11} & k_6 \\ k_3 & k_4 & k_5 & k_1 & k_8 & k_2 \\ k_5 & k_6 & k_{11} & k_8 & k_1 & k_8 \\ k_4 & k_{11} & k_6 & k_2 & k_8 & k_1 \end{bmatrix} & \mathbf{k}_6 &= \begin{bmatrix} k_{14} & k_{11} & k_7 & k_{13} & k_{10} & k_{12} \\ k_{11} & k_{14} & k_7 & k_{12} & k_9 & k_2 \\ k_7 & k_7 & k_{14} & k_{10} & k_2 & k_9 \\ k_{13} & k_{12} & k_{10} & k_{14} & k_7 & k_{11} \\ k_{10} & k_9 & k_2 & k_7 & k_{14} & k_7 \\ k_{12} & k_2 & k_9 & k_{11} & k_7 & k_{14} \end{bmatrix} \end{aligned} \quad (14)$$

where

$$\begin{aligned} k_1 &= -(6\nu-4)/9, k_2 = 1/12, \\ k_3 &= -1/9, k_4 = -(4\nu-1)/12, \\ k_5 &= (4\nu-1)/12, k_6 = 1/18, \\ k_7 &= 1/24, k_8 = -1/12, \\ k_9 &= (6\nu-5)/36, k_{10} = -(4\nu-1)/24, \\ k_{11} &= -1/24, k_{12} = (4\nu-1)/24, \\ k_{13} &= (3\nu-1)/18, k_{14} = (3\nu-2)/18 \end{aligned} \quad (15)$$

The global stiffness matrix is the collection of element stiffness matrix, which can be expressed as:

$$K(\bar{x}) = A_{i=1}^n k_i(\bar{x}_i) = A_{i=1}^n E_i(\bar{x}_i) k_i^0 \quad (16)$$

where n is the amount of elements. Based on the definition of the global stiffness matrix, Formula (16) can be further expressed as:

$$K(\bar{x}) = \sum_{i=1}^n K_i(\bar{x}_i) = \sum_{i=1}^n E_i(\bar{x}_i) K_i^0 \quad (17)$$

where K_i^0 is the global constant stiffness matrix that is composed of the element stiffness matrix. According to Formula (7), the matrix can be expressed as:

$$K(\bar{x}) = \sum_{i=1}^n [E_{\min} + \bar{x}_i^p (E_0 - E_{\min})] K_i^0 \quad (18)$$

By solving Formula (19), we can obtain the displacement vector of nodes $U(\bar{x})$.

$$K(\bar{x})U(\bar{x}) = F \quad (19)$$

where F is the force vector of nodes.

3.5 Topology Optimization Model Based on Improved SIMP method

The solution of minimum compliance problem is to find the distribution form of material density, which makes structural deformation minimum under the action of the specified load and constraint. Therefore, compliance of structure can be defined as:

$$c(\bar{x}) = F^T U(\bar{x}) \quad (20)$$

By introducing the volume restriction, the minimum compliance problem can be further expressed as follows:

$$\begin{aligned} \text{Find} \quad & x = [x_1, x_2, \dots, x_n]^T \\ \text{Minimize} \quad & c(\bar{x}) = F^T U(\bar{x}) \\ & = U^T(\bar{x}) \sum_{i=1}^n [E_{\min} + \bar{x}_i^p (E_0 - E_{\min})] K_i^0 U(\bar{x}) \\ \text{s.t.} \quad & v(\bar{x}) = \bar{x}^T v - V^* \leq 0, \\ & x \in \chi, \chi = \{x \in R^n : 0 \leq x \leq 1\} \end{aligned} \quad (21)$$

where density \bar{x} is determined by Formula (4). $v = [v_1, \dots, v_n]^T$ is the volume vector of elements.

3.6 The Sensitivity Analysis of Structure

Based on the improved SIMP model, sensitivity analysis should be indispensable in obtaining the solution to objective function.

In Formula (21), the derivative of volume constraint function $v(\bar{x})$ with respect to design variable is:

$$\frac{\partial v(\bar{x})}{\partial x_e} = \sum_{i \in N_e} \frac{\partial v(\bar{x})}{\partial x_i} \frac{\partial x_i}{\partial x_e} \quad (22)$$

where $\frac{\partial v(\bar{x})}{\partial x_i} = v_i, \frac{\partial x_i}{\partial x_e} = \frac{H_{ie} v_e}{\sum_{j \in N_i} H_{ij} v_j}$. The mesh element used in the study is the cube element with unit volume. That is, $v_i = v_j = v_e = 1$.

In Formula (21), the derivative of compliance with respect to design variable x_e is:

$$\frac{\partial c(\bar{x})}{\partial x_e} = \sum_{i \in N_e} \frac{\partial c(\bar{x})}{\partial x_i} \frac{\partial \bar{x}_i}{\partial x_e} \quad (23)$$

where

$$\frac{\partial c(\bar{x})}{\partial x_i} = F^T \frac{\partial U(\bar{x})}{\partial x_i} = U(\bar{x})^T K(\bar{x}) \frac{\partial U(\bar{x})}{\partial x_i} \quad (24)$$

In Formula (19), the derivative of total stiffness with respect to design variable \bar{x}_i is:

$$\frac{\partial K(\bar{x})}{\partial x_i} U(\bar{x}) + K(\bar{x}) \frac{\partial U(\bar{x})}{\partial x_i} = 0 \quad (25)$$

Formula (25) can be further organized as:

$$\frac{\partial U(\bar{x})}{\partial x_i} = -K(\bar{x})^{-1} \frac{\partial K(\bar{x})}{\partial x_i} U(\bar{x}) \quad (26)$$

Based on Formula (18), the equation can be expressed as:

$$\begin{aligned} \frac{\partial K(\bar{x})}{\partial x_i} &= \\ \frac{\partial}{\partial x_i} \sum_{i=1}^n [E_{min} + \bar{x}_i^p (E_0 - E_{min})] K_i^0 & \quad (27) \\ = p \bar{x}_i^{p-1} (E_0 - E_{min}) K_i^0 \end{aligned}$$

Combined with Formula (24), Formula (26) and Formula (27), it can be expressed as:

$$\frac{\partial \bar{x}}{\partial \bar{x}_i} = U(\bar{x})^T [p \bar{x}_i^{p-1} (E_0 - E_{min}) K_i^0] U(\bar{x}) \quad (28)$$

Given that K_i^0 is the collection of element stiffness matrix, Formula (28) can be expressed as:

$$\frac{\partial \bar{x}}{\partial \bar{x}_i} = u_i(\bar{x})^T [p \bar{x}_i^{p-1} (E_0 - E_{min}) k_i^0] u_i(\bar{x}) \quad (29)$$

where $u_i(\bar{x})$ is the displacement vector of element node.

Because k_i^0 is positive definite, $\frac{\partial c(\bar{x})}{\partial x_i} < 0$.

3.7 Optimization algorithm

OC method is an indirect optimization method because it does not optimize the object function directly. The method makes K-T condition, which the optimal solution should meet in math as the guideline the most optimal structure should satisfy. The outstanding characteristic is with fast convergence speed and less iteration number. The K-T condition of optimization criteria method should satisfy

$$\frac{\partial c(\bar{x})}{\partial x_e} + \lambda \frac{\partial v(\bar{x})}{\partial x_e} = 0 \quad (30)$$

where λ is Lagrangian multiplier. Formula (30) can be further expressed as:

$$B_e = -\frac{\partial c(\bar{x})}{\partial x_e} \left(\lambda \frac{\partial v(\bar{x})}{\partial x_e} \right)^{-1} \quad (31)$$

The large change of relative density from void to solid is not allowed. Therefore, moving limit m should be introduced into the design variable x . The iterative density can be further expressed as follows:

$$x_e^{new} = \begin{cases} \max(0, x_e - m), & \text{if } x_e B_e^\eta \leq \max(0, x_e - m), \\ \min(1, x_e + m), & \text{if } x_e B_e^\eta \geq \min(1, x_e + m), \\ x_e B_e^\eta & \text{otherwise} \end{cases} \quad (32)$$

where m is the moving limit. η is the damping coefficient ranging from 0 to 1. Introducing the damping coefficient and the moving limit aims to improve iteration convergence. Sigmund proposed $m=0.2$ and $\eta = 0.5$ [23]. In Formula (32), λ is the only unknown quantity. λ can be obtained in Formula (33) by dichotomy method.

$$\bar{x}^T(\lambda) - V^* = 0 \quad (33)$$

In addition, the condition that convergence rule should meet is

$$\|x^{new} - x\|_\infty \leq \mathcal{E} \quad (34)$$

where \mathcal{E} is the error limitation that is set to “0.001.”

3.8 Procedure of Obtaining Solutions

Based on MATLAB programming, we depict the whole solving flow chart shown in Figure 1 and provide specific explanations for each step.

- (1) Input of original data: maximum iteration number, material parameters (elastic modulus and Poisson ratio), coordinate of force acting point, coordinates of constraint node and freedom numbers
- (2) Definition of elemental stiffness matrix and integration of total stiffness matrix
- (3) Finite element analysis and calculation of the element nodal displacement
- (4) According to the above calculated displacement, calculating sensitivity, and objection function (compliance)
- (4) Sensitivity filtering method
- (5) To obtain the solution (Lagrange multiplier) of Formula (33) by bisection method and then obtain the new design variable density.
- (6) Convergence test is performed by Formula (34). If satisfied, the results (compliance, displacement, and nephogram of density distribution) will be the output; otherwise the solving step returns to Step 3, in which the density variable is updated to perform the finite element analysis.

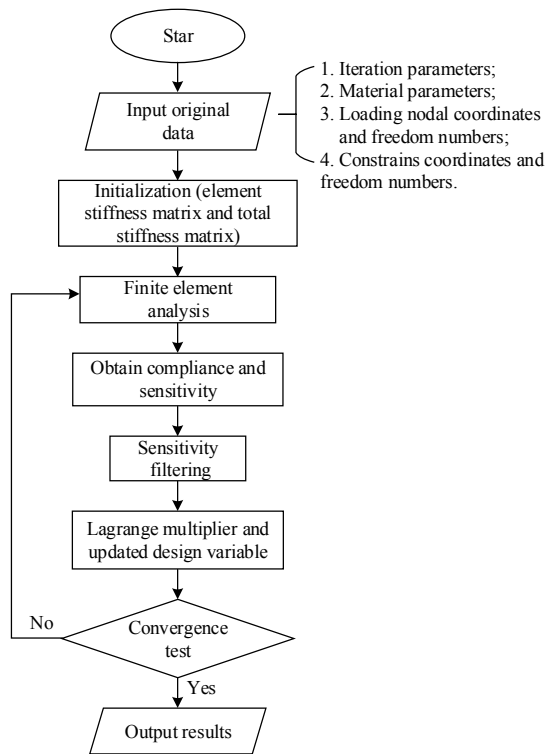


Fig.1. Solving flow chart of 3D continuum structure topology optimization

4. Result Analysis and Discussion

4.1 Example Verification

As is shown in Figure 2, the design domain is a 3D continuum cantilever beam with reserved hole. The length in x direction is 40 mm; the width in y direction is 20 mm; and the thickness in z direction is 10 mm. A cylinder hole with radius of 7 mm is in the center of the entire structure. The discrete structure is partitioned into 32×16×8 hexahedral elements. The left side boundary condition is fully fixed and the right side at the bottom of the beam is subjected to a concentrated line load 1 kN/m. The elastic modulus of material $E_0 = 1$ GPa, the volume fraction is 0.3, the penalty factor $p=3.0$, and the filtering radius $r=1.5$. The objective

function is to minimize the compliance of the entire structure. The iteration results are shown in Table 1.

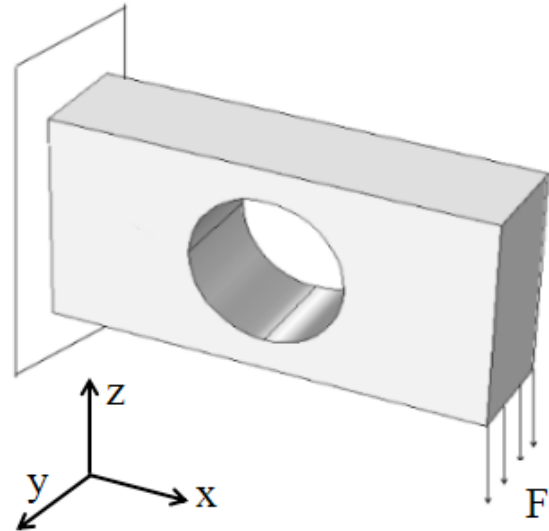


Fig. 2. Initial design domain of the 3D continuum cantilever beam

Table 1 presents the topology optimization results in the iteration process. From the table, we can see that when the iteration step reaches step 5, the shape of the topology structure is unformed. When the iteration process reaches step 50, the structure is fully shaped into many supporting bars in the local region. With the increase of iteration numbers, the structure form has only a subtle change.

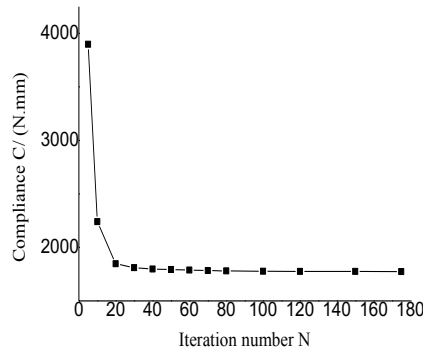
To reflect the change trend of compliance, maximum displacement, and density index with the increase of the iteration numbers, Figures 3(a), (b), (c) are drawn respectively. Herein, the density index is defined as the ratio of element numbers of which density is less than 0.01 and greater than 0.99 to the total element numbers. This index reflects the extent that the whole element density tends to be 0 or 1. When the iteration number begins to reach 20, the compliance and the maximum displacement decline sharply, whereas the density index climbs rapidly. As the iteration number continues to increase, all the results (compliance and maximum displacement) have only subtle changes. From the above density nephogram change and iteration results of various index, we can conclude that the presented numerical method is stable, reasonable, and with good convergence.

Table 1. Topology optimization results in the process of iterations

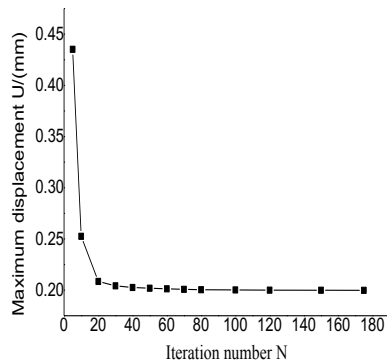
Iteration numbers	5	10	20	50	100	175
3D cubic nephogram						
Side-view nephogram						

Note:

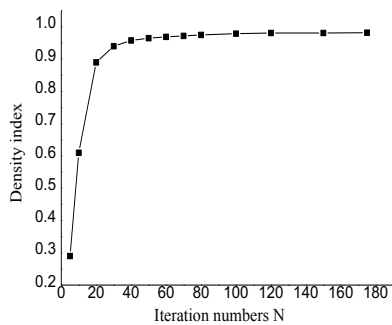
is density scale, which is applicable to all the density nephogram in this study.



(a) Compliance



(b) Maximum displacement



(c) Density index

Fig. 3. Variation of compliance, maximum displacement, and density index with iteration numbers

4.2 Mesh Dependency Analysis

To analyze the influence of element numbers on optimization results and computation time, five cases with mesh numbers $16 \times 8 \times 4$, $20 \times 10 \times 5$, $32 \times 16 \times 8$, $40 \times 20 \times 10$, $48 \times 24 \times 12$ are discussed. The penalty factor is $p=3.0$ and filtering radius is $r=1.5$.

From Table 2, we can see that if the mesh numbers are too coarse or too fine, the calculated compliance and the maximum displacement are both too large. In special cases, when the mesh is $32 \times 16 \times 8$, the optimal compliance is the minimum in five cases. As the mesh numbers increase, iteration steps increase and computation time becomes longer. Meanwhile, the density index becomes larger, that is, the element number ratio of the intermediate density decreases. In addition, the mesh numbers do not affect the structure form significantly. Based on overall consideration of the optimization results and calculating cost, the reasonable mesh numbers in this study are $32 \times 16 \times 8$.

4.3 Penalty Factor Analysis

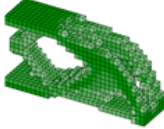
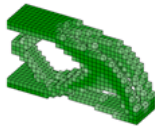
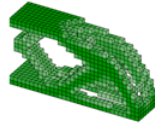
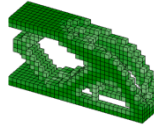
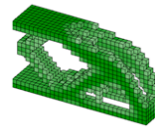





To analyze the influence of different penalty factors on the optimization results and computation time, we studied five cases with penalty factors 2.0, 2.5, 3.0, 3.5, and 4.0. Herein, the mesh number is $32 \times 16 \times 8$ and filtering radius $r=1.5$ in five cases.

As is shown in Table 3, with the increase of penalty factor, the calculated compliance, maximum displacement, and density index become larger. Furthermore, when the penalty factor is non-integer, iteration steps grow apparently and computation cost increases. When the penalty factor is an integer, the iteration number is relatively small, and the larger the penalty factor is, the faster the convergence time will be. However, the optimal compliance and the maximum displacement both increase, which suggests that the optimization effect declines. Based on an overall consideration of optimization results and calculating cost, the reasonable penalty factor in this example should be 3.0.

Table 2. Final topology optimization results of different numbers of mesh elements

Mesh partition	$16 \times 8 \times 4$	$20 \times 10 \times 5$	$32 \times 16 \times 8$	$40 \times 20 \times 10$	$48 \times 24 \times 12$
Iteration step	49	159	175	170	475
Compliance (N · m)	1836.01×10^{-3}	1787.01×10^{-3}	1774.25×10^{-3}	1931.22×10^{-3}	2077.22×10^{-3}
Maximum displacement (m)	0.2345×10^{-3}	0.2267×10^{-3}	0.1998×10^{-3}	0.2400×10^{-3}	0.2530×10^{-3}
Density index	0.9219	0.9450	0.9819	0.9915	0.9942
3D view nephogram					
Side-view nephogram					

Table 3. Final topology optimization results of different penalty factors

Penalty factor	2.0	2.5	3.0	3.5	4.0
Iteration step	285	249	175	315	178
Compliance (N·m)	1472.35×10^{-3}	1635.32×10^{-3}	1774.25×10^{-3}	1895.25×10^{-3}	2006.01×10^{-3}
Maximum displacement (m)	0.1649×10^{-3}	0.1835×10^{-3}	0.1998×10^{-3}	0.2158×10^{-3}	0.2270×10^{-3}
Density index	0.9663	0.9824	0.9819	0.9888	0.9917
3D view nephogram					
Side-view nephogram					

4.4 Filtering Radius Analysis

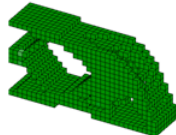
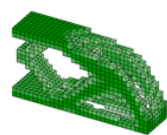
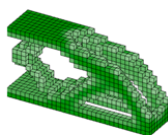
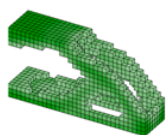


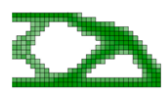
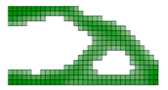
To analyze the influence of different filtering radius on the optimization results and computation time, four cases with the filtering radius 1, 1.5, 2.0, 3.5 are discussed. Herein, the mesh number is $32 \times 16 \times 8$ and penalty factor $p=2.0$ in five cases.

Table 4 shows that with the increase of filtering radius, compliance, maximum displacement, iteration number

increase. When filtering radius is 1.0, the local region of the structure appears as chessboard phenomenon.

As the filtering radius is larger than 1.0, the optimal structure form no longer appears as a chessboard problem. When filtering radius is too large or too small, the density index will increase. As the filtering radius is 3.5, the shape of the structure changes sharply. Meanwhile, the compliance and the maximum displacement of structure become larger. Based on overall consideration of results and calculating cost, the reasonable filtering radius in this example is 1.5.

Table 4. Final topology optimization results of different filtering radius

Filtering radius	1.0	1.5	2.0	3.5
Iteration step	22	175	261	306
Compliance (N·m)	1472.35×10^{-3}	1774.25×10^{-3}	2059.27×10^{-3}	3096.51×10^{-3}
Maximum displacement (m)	0.1649×10^{-3}	0.1998×10^{-3}	0.2331×10^{-3}	0.3510×10^{-3}
Density index	0.9663	0.9819	0.9790	0.9800
3D view nephogram				
Side-view nephogram				

5. Conclusion

In this study, the topology optimization model of 3D continuum structure with objective function of minimum compliance and design variable of material distribution is established. By introducing the sensitivity filtering method and the improved SIMP model, the OC iteration equation of finite element analysis is deduced. By MATLAB programming, the 3D continuum structure with reserved hole is designed to obtain optimal topology structure shape. Based on the above analysis, we obtain the following conclusions:

(1) Compared with the previous topology optimization of 2D continuum structures, the presented method of topology optimization of 3D continuum structure with reserved hole can enlarge the application for more complicated structures.

(2) Too fine or too coarse mesh number will greatly make the compliance and the maximum displacement larger. In addition, the finer the mesh is, the more the iteration step is, and the computation cost will increase. Meanwhile, the density index will become larger, which means that the intermediate density decreases. Furthermore, the mesh number affects the shape form of structure less.

(3) As the filtering radius is larger than 1.0, the topology shape will no longer appear as a chessboard problem, which suggests that the presented sensitivity filtering method is valid. However, the larger the filtering radius is, the longer the computation time will be. Therefore, selecting an appropriate filtering radius can not only improve the optimal effect but also save the computation cost.

(4) The penalty factor should be an integer because the iteration step increases greatly when the value is a non-integer.

References

1. Michell A G M., "The limit of economy of material in frame structures". *Philosophical Magazine*, 8(6), 1904, pp. 589-597.
2. Dorn W., Gomory R., Greenberg H., "Automatic design of optimal structures". *Design Magazine*, 3(1), 1964, pp. 25-52.

3. Bendsoe, Kikuchi, "Optimal topologies in structural design using a homogenization method", *Computer Methods in Applied Mechanics and Engineering*, 71(2), 1988, pp. 197-224.
4. Sigmund O, Maute K. "Topology optimization approaches". *Structural & Multidisciplinary Optimization*, 48(6), 2013, pp. 1031-1055.
5. BH Wu., BJ Pang., ZQ Deng., "Topological optimization of pedestal based on variable density method", *Key Engineering Materials*, 568(7), 2013, pp. 109-113.
6. Yang R J., Chuang C H., "Optimal topology design using linear programming", *Computers and structures*, 52(2), 1994, pp. 265-275.
7. P Zhang., J Toman., Y Yu., E Biyikli., M Kirca., "Efficient design-optimization of variable-density hexagonal cellular structure by additive manufacturing: theory and validation", *Journal of Manufacturing Science & Engineering*, 137(2), 2015, pp. 021004..
8. Zhou Y, Fei Q. "Dynamic design of stiffeners for a typical panel using topology optimization and finite element analysis". *Advances in Mechanical Engineering*, 7(3), 2015, pp. 1687814015572465.
9. BH Wu., BJ Pang., ZQ Deng., "Topology optimization in support of space borne device based on variable density method", *Key Engineering Materials*, 568(1), 2013, pp. 109-113.
10. P Li., L Zheng., Z Fang., "Topology optimization of constrained layer damping structure based on SIMP interpolation method", *Mechanical Science & Technology for Aerospace Engineering*, 33(8), 2014, pp. 1122-1126.
11. ZHU J, JIANG L. "Multi-level Optimization of Concrete Frames with Steel Braces". *Structural Engineers*, 29(5), 2013, pp. 007.
12. Zhu Jiejiang., Dai Lijuan., Jiang Liang., "Optimization of concrete frame with steel brace", *Building Science Research of Sichuan*, 40(4), 2014, pp. 7-25.
13. J Zhu., Y Lin, X., Chen, G Shi., "Research on improved sensitivity modification method of continuum topology optimization", *China Mechanical Engineering*, 25(11), 2014, pp. 1506-1510.
14. Sigmund O., Petersson J., "Numerical instabilities in topology optimization: a survey on procedures dealing with checkerboards mesh-dependencies and local minima", *Structural Optimization*, 16(1), 1998, pp. 68-75.
15. Zuo K T., Chen L P., Zhang Y O., "Study of key algorithms in topology optimization", *International Journal of Advanced Manufacturing Technology*, 32(7), 2007, pp. 787-796.
16. Long Kai. Zuo Zhengxing., Xiao Tao., "Research on filter algorithm applied in continuum topology optimization," *China Mechanical Engineering*, 18(10), 2007, pp. 1171-1174.
17. D Lee., CN Hong., S Shin., "Generation of OC and MMA topology optimizer by using accelerating design variables", *Structural Engineering & Mechanics*, 55(5), 2015, pp. 901-911.
18. Schmit L A., "Structural design by systematic synthesis," *Proc. 2nd Conf. Electronic Computation, ASCE*, 32(1) 1960, pp. 105-132.
19. N Manavizadeh., NS Hosseini., M Rabbani., F Jolai., "A simulated annealing algorithm for a mixed model assembly U-line balancing type-I problem considering human efficiency and Just-In-Time approach", *Computers & Industrial Engineering*, 64(2), 2013, pp. 669-685.
20. FY Cheng., D Li., "Multi-objective optimization design with genetic algorithm", *Journal of Structural Engineering*, 123(9), 1997, pp. 1252-1261.
21. AB Ruiz., R Saborido., M Luque., "A preference-based evolutionary algorithm for multi-objective optimization: the weighting achievement scalarizing function genetic algorithm", *Journal of Global Optimization*, 62(1), 2015, 101-129.
22. AA Seleemah., "A neural network model for predicting maximum shear capacity of concrete beams without transverse reinforcement", *Canadian Journal of Civil Engineering*, 32(4), 2005, 644-657.
23. Li Z, Kan G, Yao C, et al. "Improved Neural Network Model and Its Application in Hydrological Simulation". *Journal of Hydrologic Engineering*, 19(10), 2013, pp. 04014019.
24. A Walther, L Biegler., "On an inexact trust-region SQP-filter method for constrained nonlinear optimization", *Computational Optimization & Applications*, 63(3), 2016, pp. 1-26.
25. Zhu Jiejiang., Sun Yuming., "Space steel frame optimization based on the sequence linear programming", *Structural Engineering*, 30(6), 2014, pp. 25-32.
26. Z Ling., X Ronglu., W Yi., A El-Sabbagh., "Topology optimization of constrained layer damping on plates using Method of Moving Asymptote (MMA) approach", *Shock & Vibration*, 18(1-2), 2011, pp. 221-244.
27. L Li., K Khandelwal., "Two-point gradient-based MMA (TGMA) algorithm for topology optimization", *Computers & Structures*, 131(2), 2014, pp. 34-45.
28. Sigmund O., "Morphology-based black and white filters for topology optimization", *Structural & Multidisciplinary Optimization*, 33(4), 2007, pp. 401-424.